



Observation of spontaneous orientation polarization in evaporated films of organic light-emitting diode materials

Kohei Osada^a, Kenichi Goushi^b, Hironori Kaji^c, Chihaya Adachi^b, Hisao Ishii^{d,e,*},
Yutaka Noguchi^{a,**}

^a School of Science & Technology, Meiji University, Kawasaki, Japan

^b Center for Organic Photonics and Electronics Research, Kyushu University, Fukuoka, Japan

^c Institute for Chemical Research, Kyoto University, Kyoto, Japan

^d Center for Frontier Science, Chiba University, Japan

^e Graduate School of Advanced Integration Science, Chiba University, Chiba, Japan

ARTICLE INFO

Keywords:

Organic light-emitting diodes
Molecular orientation
Permanent dipole moment
Spontaneous orientation polarization
Giant surface potential

ABSTRACT

The molecular orientation in organic semiconductor films determines device performances. In particular, the spontaneous orientation of a permanent dipole moment (PDM) along the surface normal direction induces a polarization charge at the hetero-interfaces of stacked multilayer devices, and the interface charge dominates the charge accumulation and injection properties. Spontaneous orientation polarization (SOP) has been observed in the “randomly oriented” films of several organic semiconductor materials, and is potentially inherent in many common materials. Herein, we report that 11 additional molecules of organic light-emitting diode materials, including thermally activated delayed fluorescence emitters, and horizontally oriented emitters and electron transporters, exhibit SOP in their evaporated films. The experimental results clearly indicate that SOP frequently occurs in “horizontally oriented” films as well as “randomly oriented” films. The factors contributing to SOP formation are discussed in terms of the figure of merit per PDM. We found that strong intermolecular interactions tend to reduce the figure of merit. Moreover, we suggest the impact of SOP on device performances.

1. Introduction

Molecular orientation in amorphous organic films has attracted much attention because it influences the resultant electrical and optical properties of devices [1–5]. In organic light-emitting diodes (OLEDs), the horizontal orientation of the emitter's transition dipole moment (TDM) has been found to enhance light outcoupling [2,6–8], and π -stacking along the surface normal direction has been reported to improve the charge transport characteristics [1,9,10]. Spontaneous orientation polarization (SOP) originating from the orientation of the permanent dipole moment (PDM) in evaporated films [11] induces a polarization charge at the hetero-interface, which dominates the charge injection and accumulation behaviors of multilayer devices [4,5]. Moreover, interface charge density has been correlated with luminous efficiency degradation in archetypal OLEDs [12–15]. To understand and control the molecular orientation in devices, which is essential for optimizing device performances, several researchers have designed the molecular structure of OLED materials and investigated the film formation conditions [10,16–20]. However, the driving force of

anisotropic molecular orientation is incompletely understood, and the manipulation of molecular orientation in actual devices is a challenging problem.

Molecular orientation in films has been typically estimated using optical techniques, such as variable angle spectroscopic ellipsometry [1] and angular dependent photoluminescence measurements [2], which measure the orientation of the TDM intensity. The order parameter S evaluated by these methods is given by

$$S = \frac{3\langle \cos^2 \theta_t \rangle - 1}{2} \quad (1)$$

where θ_t is the TDM angle with reference to the surface normal, and S varies from -0.5 (horizontal orientation) to 1.0 (vertical orientation). Conversely, SOP has been evaluated by measuring the surface potential of the organic films as a function of film thickness (by the Kelvin probe method) and accumulated charge density at the hetero interface in the device structures (using displacement current measurements or impedance spectroscopy) [4,19]. The molecular orientations in films with SOP have also been evaluated by nonlinear optical measurements

* Corresponding author. Center for Frontier Science, Chiba University, Japan.

** Corresponding author. School of Science & Technology, Meiji University, Kawasaki, Japan.

E-mail addresses: ishii130@faculty.chiba-u.jp (H. Ishii), noguchi@meiji.ac.jp (Y. Noguchi).

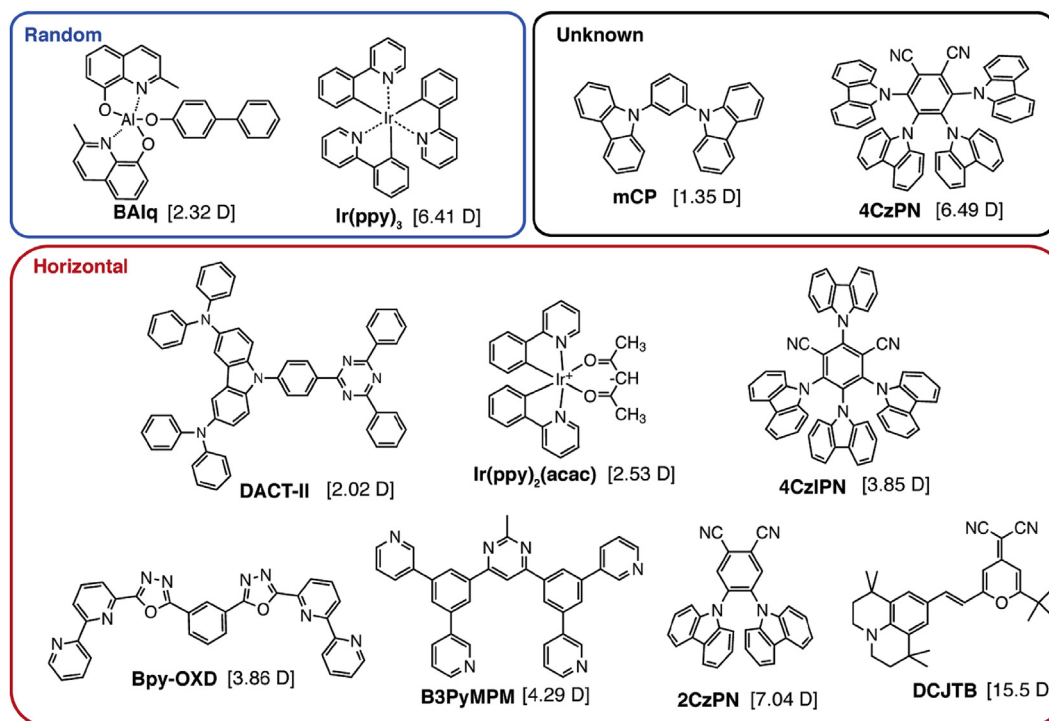


Fig. 1. Molecular structures of the organic materials used in this study. The PDM of each molecule was calculated by quantum chemical calculations using DFT/B3LYP with a LANL2DZ basis set for Ir(ppy)₃ and Ir(ppy)₂(acac), and a 6-31G* basis set for all other molecules. The molecules were divided into three classes (random, unknown, and horizontal) based on their reported TDM orientations.

[21,22].

SOP originates from the PDM of the molecule, which is partially piled up along the surface normal direction of the film. If the PDM orientation is constant on average, the surface potential increases linearly as a function of film thickness without saturation. The surface potential typically exceeds the energy gap between the highest occupied molecular orbital and the lowest unoccupied molecular orbital (HOMO–LUMO gap) of the molecule at a film thickness of around 100 nm. In 1972, Kutzner reported such unusual build-ups of the surface potential in gases condensed on a cold surface below 100 K [23]. Since then, the spontaneous polarization of the condensates of water ice, alcohols, ketones, ethers, and other materials have been widely investigated [24–29]. In 2002, Ito et al. found a similar phenomenon in a typical organic semiconductor film deposited at room temperature, which they called the giant surface potential (GSP) [11]. The GSP (V_s) is proportional to SOP and given by

$$V_s = \frac{P_0 \cdot \hat{z}}{\epsilon} d = \frac{p \langle \cos \theta_p \rangle n}{\epsilon} d, \quad (2)$$

where P_0 is the spontaneous polarization vector, \hat{z} is the surface normal vector, ϵ is the dielectric constant, d is the film thickness, p is the intensity of PDM, $\langle \cos \theta_p \rangle$ indicates the average contribution of p to the surface normal direction, and n is the molecular density. Although GSP originates from PDM orientation, the terms “random” and “horizontal” orientation throughout this paper refer to TDM orientation. Typically, the GSP slope (V_s/d) is several tens of mV/nm [4,11,30], and this value is comparable to the electric field formed in operating OLEDs. Consequently, the GSP influences the device properties of the OLED [4,5,14].

SOP has been observed in the evaporated films of several OLED materials, but the mechanism of SOP formation remains to be clarified. Interestingly, all of these films are so called “randomly oriented” films in terms of TDM. In the typical optical measurements, the head and tail of the molecule are indistinguishable because these methods evaluate the orientation of TDM intensity ($\propto \langle \cos^2 \theta_t \rangle$). Moreover, random TDM orientation does not necessarily indicate random orientation of the

symmetry axis of the molecule. For example, Murawski et al. recently reported that the molecular orientation in the tris(2-phenylpyridine) iridium(III) (Ir(ppy)₃) film, which has a random TDM orientation [31]. On the other hand, SOP originates from the PDM orientation including its head-to tail-direction, as it is proportional to $\langle \cos \theta_p \rangle$. The SOP is therefore inherent even in “randomly oriented” films. In contrast, “horizontally oriented” films have not been examined for SOP. Whether and how SOP appears in “horizontally oriented” films is important for understanding the mechanism of SOP formation and for accurately evaluating the molecular orientation.

In this study, we divide typical OLED materials into “random,” “horizontal,” and “unknown” based on their TDM orientation, and measure the surface potentials of their evaporated films. We find the typical GSP behavior in the films of horizontally oriented emitters and electron transporters, including thermally activated delayed fluorescence (TADF) emitters [32,33]. The contributing factors of SOP formation are discussed in terms of the figure of merit of the GSP slope per PDM. In this analysis, we find that strong intermolecular interactions tend to reduce the figure of merit. Our experimental results clearly indicate that SOP is very common in the organic semiconductor films of polar molecules, and contributes to revealing the mechanism of spontaneously formed molecular orientation.

2. Experimental

Fig. 1 shows the structure of the molecules used in this study. The horizontal TDM orientation is known for evaporated films of the following molecules: 4-[dicyanomethylene]-2-*tert*-butyl-6-(1,1,7,7-tetramethyljulolidyl-9-enyl)-4H-pyran (DCJTb) [34], 1,2-bis(carbazol-9-yl)-4,5-dicyanobenzene (2CzPN) [35], bis-4,6-(3,5-di-3-pyridylphenyl)-2-methylpyrimidine (B3PyMPM) [9], 1,3-bis[2-(2,2'-bipyridine-6-yl)-1,3,4-oxadiazol-5-yl]benzene (Bpy-OXD) [36], 1,2,3,5-Tetrakis(carbazol-9-yl)-4,6-dicyanobenzene (4CzIPN) [37], bis[2-(2-pyridinyl-N)phenyl-C](acetylacetonate) iridium(III) (Ir(ppy)₂(acac)) [8,16,17,38], and 9-[4-(4,6-diphenyl-1,3,5-triazin-2-yl)phenyl]-N,N,N',N'-tetraphenyl-9H-carbazole-3,6-diamine

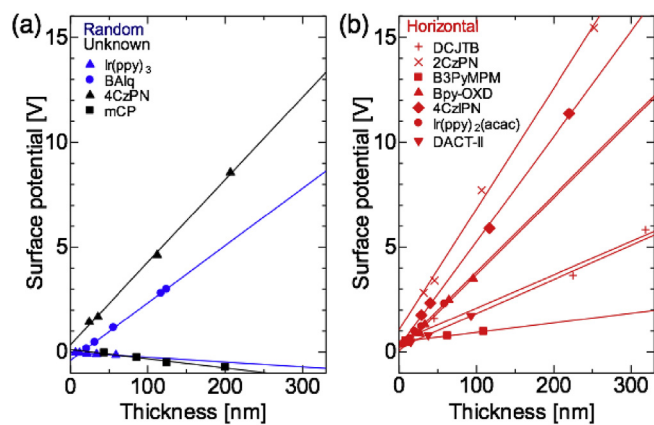


Fig. 2. Surface potentials of evaporated organic films as a function of film thickness. (a) “Random” and “Unknown” materials. (b) “Horizontal” materials.

(DACT-II) [32]. Although the TDM orientations of some of these materials have been measured in doped film, similar qualitative orientations are expected in neat films [1,31,39]. We divided the materials into three groups with different qualitative TDM orientations, namely, random, unknown, and horizontal (Fig. 1). p of each molecule in the optimized structure was calculated using density functional theory (DFT, B3LYP) in Gaussian 16. The basis set was LANL2DZ for Ir(ppy)₃ and Ir(ppy)₂(acac), and 6-31G* for all other molecules. As some molecules exhibit several conformers, the conformers of each molecule were searched through a molecular dynamics simulation, and the optimized structure was calculated by DFT for each conformer. p at the minimum energy among the conformers is used in this study. The molecular structures at the minimum energy are shown in Fig. S1.

Indium–tin–oxide (ITO) coated glass substrates were successively sonicated in detergent (10 min, once), pure water (5 min, four times), acetone (5 min, twice), and isopropyl alcohol (5 min, twice). The substrates were then exposed to ultraviolet-ozone treatment for 10 min. Organic layers were deposited on one half of the substrate through a shadow mask by a conventional vacuum evaporation technique at a base pressure of $\sim 10^{-4}$ Pa in the dark. The deposition rate of each organic layer was 0.3–2 Å/s. The substrate temperature was not controlled during the film deposition. The film thickness of each layer ranged from 5 to 300 nm. The samples were kept in the dark or under red light (peak wavelength: 640 nm, FWHM: 25 nm) to avoid the generation of photocarriers in the film, which would decay the surface potential [10]. Sublimed-grade organic semiconductors (except for the TADF emitters) were purchased from Lumtec Corp. and used without further purification. 2CzPN, 1,2,3,4-tetrakis(carbazol-9-yl)-5,6-dicyanobenzene (4CzPN), and 4CzIPN were synthesized and purified by the Adachi group at Kyushu University, and DACT-II was synthesized and purified by the Kaji group at Kyoto University.

The surface potential was measured by the Kelvin probe method (Trek 320C with a 3250-V probe) under a pressure of $\sim 10^{-4}$ Pa in the dark. The samples were exposed to air while transferring them from the evaporation chamber to the measurement chamber. The surface potential on the organic films was measured as a function of the film thickness with reference to the ITO substrate. The film thickness was finally measured using a stylus profilometer (Dektak 6 M) or an atomic force microscope (Bruker MultiMode8).

3. Results and discussion

Fig. 2(a) displays the surface potentials of the “random” and “unknown” materials, *i.e.*, bis(2-methyl-8-quinolinolate)-4-(phenylphenolato)aluminum (BALq) [40], Ir(ppy)₃ [38], 4CzPN, and 1,3-Bis(N-carbazolyl)benzene (mCP), as a function of film thickness. The evaporated films of all materials exhibit GSP behavior, *i.e.*, linear growth of the

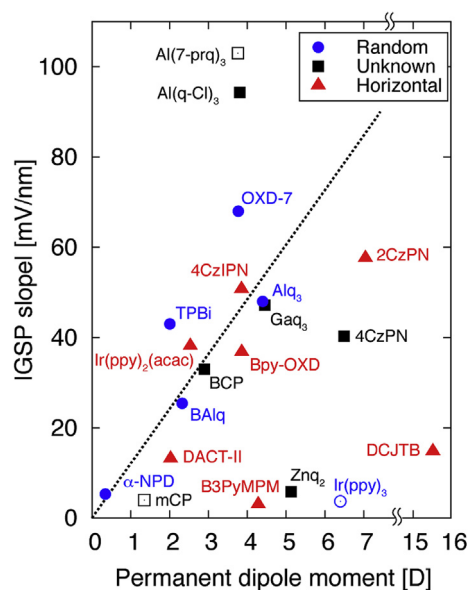


Fig. 3. Relationship between the absolute value of GSP slope and p for various organic materials. Alq₃: tris(8-hydroxyquinoline)aluminum (III), TPBi: 1,3,5-tris(1-phenyl-1H-benzimidazol-2-yl)benzene, BCP: 2,9-dimethyl-4,7-diphenyl-1,10-phenanthroline, OXD-7: 1,3-bis[2-(4-*tert*-butylphenyl)-1,3,4-oxadiazol-5-yl]benzene, Al(7-prq)₃: tris(7-propyl-8-hydroxyquinolinolato)aluminum(III), Znq₂: bis(8-hydroxyquinoline)zinc, Gaq₃: tris(8-hydroxyquinolinato)gallium (III), Al(q-Cl)₃: tris(5-chloro-8-hydroxyquinolinato)aluminum. Each symbol indicates the TDM orientation in evaporated films with random (blue circles), unknown (black squares), and horizontal (red triangle) molecular orientations. Open symbols indicate negative GSP. The data of Alq₃, TPBi, BCP, OXD-7 [4], Al(7-prq)₃ [5,20], Znq₂, Gaq₃, and Al(q-Cl)₃ [30] were obtained from the literature. Note that the GSP slope for DCJTb was variable probably depending on the details of the film formation conditions, though the linearity was observed in all sets of samples. We observed the GSP slope for DCJTb from 7 to 25 mV/nm, and the average was 14.8 mV/nm. For TPBi, a larger GSP is also reported (~ 70 mV/nm) [41]. The broken line denotes the average slope of all materials except for those with extremely high (Al(7prq)₃, Al(q-Cl)₃) or low (DCJTb, Ir(ppy)₃, Znq₂, B3PyMPM, mCP) figures of merit. (For interpretation of the references to colour in this figure legend, the reader is referred to the Web version of this article.)

surface potential with a constant slope, indicating the presence of SOP. In the BALq and 4CzPN films, the surface potential exceeds the HOMO–LUMO gap at film thicknesses over ~ 100 nm. These behaviors correspond to the typical characteristics of GSP reported previously [4,11,30]. On the other hand, the Ir(ppy)₃ and mCP films exhibit a weak and negative GSP.

Fig. 2(b) shows the surface potentials of the horizontally oriented materials, *i.e.*, DCJTb, 2CzPN, B3PyMPM, Bpy-OXD, 4CzIPN, Ir(ppy)₂(acac), and DACT-II, as a function of film thickness. As these molecules exhibit significant TDM orientations, some intermolecular interactions in these films are expected to be greater than those in the random orientation films. Nevertheless, these materials except for B3PyMPM exhibit typical GSP behavior, indicating that GSP is very common in “horizontally oriented” films as well as “randomly oriented” films.

Fig. 3 plots the absolute value of the GSP slope versus the dipole moment p for films in our study and in previous studies [4,5,11,20,30,41]. We note here that Fig. 3 includes the GSP slopes of the films formed on different substrates, *e.g.*, Au and organic films; however, the influence of the substrate on GSP slope is considered to be small except for the case of reactive metals (K, Ca, Mg) [4,20,30,42]. Thus we discuss the trend of the GSP slope in Fig. 3. Although the plots in Fig. 3 are widely distributed, the GSP slope is generally large for large PDM molecules.

The broken line in Fig. 3 indicates the average slope ($n\langle \cos \theta_p \rangle / \epsilon$), excluding materials with extremely high slope (Al(7prq)₃, Al(q-Cl)₃) or

low slope (DCJTb, Ir(ppy)₃, Znq₂, B3PyMPPM, mCP). The slope is considered to measure the efficiency of SOP formation per PDM, and $\eta = n \langle \cos \theta_p \rangle / \varepsilon$ is defined as the figure of merit. Interestingly, several materials, such as Alq₃, BCP, Bpy-OXD, and Ir(ppy)₂(acac), plot close to the average slope, indicating that these materials form SOPs with similar efficiencies despite being classified as “randomly oriented” or “horizontally oriented” films.

Several materials (DCJTb, Ir(ppy)₃, Znq₂, B3PyMPPM, and mCP) exhibit an extremely small η . For molecules with relatively large PDM or small size (DCJTb, Ir(ppy)₃, Znq₂, mCP), a small η implies a contribution from dipole–dipole interaction ($\propto p^2/r^3$, where r is the intermolecular distance). The electrostatic energy density in the film ($\varepsilon(V_s/d)^2/2 = \varepsilon\eta^2 p^2/2$) is reduced by forming anti-parallel PDM configurations [19], and the anti-parallel configuration neutralizes the contribution of PDM, leading to a small SOP. In the case of B3PyMPPM, a strong interaction due to intermolecular hydrogen bonding was reported [10]. The strong in-plane intermolecular interactions induce a planer structure that reduces the PDM and the out-of-plane anisotropies in the resultant films; consequently, the SOP is negligible. SOP formation appears to be driven by a combination of several factors, such as electrostatic interactions [19], surface free energy [16], and asymmetric molecular shape [20]. Although the comprehensive mechanism has not been clarified, the results imply a negative contribution of intermolecular interactions.

To confirm the contribution of intermolecular interactions, the interaction energies of the dimers with different intermolecular distances were roughly estimated using Gaussian 16 with counterpoise corrections [43,44]. The interaction energies were calculated as the difference between the total energy of two isolated molecules and the energy of the dimer. The counterpoise method handles the basis set superposition error by calculating each unit including only the basis functions (“ghost orbitals”) of the other unit. The structure of each molecule was fixed at the optimized structure of the isolated molecule. The PDM of the two molecules was maintained in an anti-parallel form (see Fig. S2 in the Supporting Information) while the intermolecular distance was varied from ~5 to 30 Å, and the single-point energies were calculated for each configuration. Note that DFT (B3LYP) with a basis set of 6-31G* or LANL2DZ is used for the calculations and dispersion forces are omitted since we focus on the electrostatic interactions.

Fig. 4 shows the calculated intermolecular interactions of the selected molecules. The calculation results of the other molecules are presented in the Supporting Information (Fig. S3). As evidenced in Fig. 4, the DCJTb, Ir(ppy)₃, Znq₂, and B3PyMPPM dimers have particularly strong interaction energies (comparable to or exceeding the thermal energy at room temperature). These molecules correspond to molecules with extremely small η (Fig. 3). Although the calculations were only rough estimates, strong electrostatic forces are likely to reduce η . We note here that mCP has a weak intermolecular interaction despite its extremely small η [Fig. S3(a)]. Similarly, the minimum interaction energy of each dimer is not of the order of η (Fig. S3). These results indicate that intermolecular interaction is not the sole mechanism to reduce η and other factors including the driving force of SOP formation should be considered.

In contrast, TPBi, OXD-7, Al(q-Cl)₃, and Al(7-prq)₃ show relatively large η . In these molecules, certain factors should drive the efficient formation of SOP along the surface-normal direction. Jurow et al. proposed a mechanism of molecular alignment for heteroleptic phosphors similar to Ir(ppy)₂(acac) [16]. In this mechanism, the boundary between the organic film surface and vacuum created during deposition induces the orientation of asymmetric molecules, thereby reducing the surface-free energy. Similarly, Isoshima et al. proposed the “asymmetric dice model” to explain the SOP formation of Alq₃ and Al(7-prq)₃ films [20]. According to this model, SOP originates from the biased distribution of stable postures of the molecules on the film surface. In both models, the molecular shape with respect to the PDM vector is crucially important. However, looking at the molecules exhibiting the large or

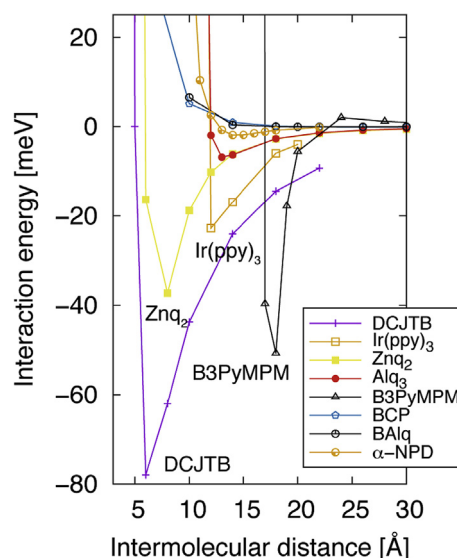


Fig. 4. Calculated intermolecular interaction energies of dimers of selected molecules. The permanent dipole moment of the two molecules in each dimer was arranged in anti-parallel form (Fig. S2 in Supporting Information). The interaction energies of each dimer with counterpoise corrections were calculated DFT in Gaussian 16, using the LANL2DZ basis set for Ir(ppy)₃, and the 6-31G* basis set for all other molecules. The molecules in this plot appear near the average slope in Fig. 3, or exhibit particularly strong interaction energies. The calculation results of the other molecules are shown in Fig. S3.

similar η , consistent characteristics of its molecular shape have not been found (Fig. 3 and Fig. S1). Further investigations are required to reveal the driving force of SOP formation.

Finally, we briefly comment on how SOP affects device performances. The SOP of the electron transporting materials between the emission layer and the cathode is expected to be important for improving the device performances. It has been reported that a positive SOP can assist electron injection from the cathode to the film, because of positive polarization charge at the interface [5,45,46]. Hence, a positive SOP should enable efficient electron injection into the Alq₃, OXD-7, Bpy-OXD, BCP, TPBi, and BAQ films. The SOP also contributes to device properties by accumulating charge at the emitter side of the electron transport layer. A positive SOP of the electron transport layer induces a negative polarization charge at the emission layer side. Negative polarization charge behaves as a hole reservoir [47], so a high charge recombination rate is expected at the interface of electron transport layer and emission layer [12–14,48]. Although this effect can improve the internal quantum efficiency of a pristine device, the charge concentration in the recombination zone leads to fast degradation [49]. Therefore, a broad interface, which can be formed by intermixing the emission layer with an electron transport layer, improves the device stability [50] by diluting the polarization charge density, and consequently the exciton concentration. As most electron transport materials exhibit SOP, the polarization charges at the interfaces should be optimized for high device performances.

4. Conclusions

In summary, we identified GSP in the evaporated films of eleven materials, including TADF emitters, and horizontally oriented emitters and electron transporters. Our experimental results clearly indicate that SOP commonly occurs in both “randomly” and “horizontally oriented” films. Since most electron transport materials exhibit SOP, the presence of polarization charge at the interfaces should be considered to optimize device performances. Although the mechanism of SOP formation has not been comprehensively explained, strong intermolecular interactions probably reduce the figure of merit of GSP. DFT calculations of

intermolecular interaction of dimers are useful for exploring materials with extremely small figures of merit. Very recently, Friederich et al. demonstrated a molecular simulation protocol that mimics the spontaneous build-up of GSP [51]. Their results are basically consistent with our results.

Acknowledgements

We would like to thank Assoc. Prof. Daisuke Yokoyama (Yamagata University) for providing molecular orientation data and fruitful discussions. This work was partly supported Japan Society for the Promotion of Science Grant-in-Aid for Scientific Research (A) (No. 17H01231). The quantum chemical calculations were partly performed using Research Center for Computational Science, Okazaki, Japan.

Appendix A. Supplementary data

Supplementary data related to this article can be found at <http://dx.doi.org/10.1016/j.orgel.2018.04.026>.

References

- [1] D. Yokoyama, *J. Mater. Chem.* 21 (2011) 19187.
- [2] W. Brütting, J. Frischeisen, T.D. Schmidt, B.J. Scholz, C. Mayr, *Phys. Status Solidi* 210 (2013) 44.
- [3] M.C. Gather, S. Reineke, *J. Photon. Energy* 5 (2015) 57607.
- [4] Y. Noguchi, Y. Miyazaki, Y. Tanaka, N. Sato, Y. Nakayama, T.D. Schmidt, W. Brütting, H. Ishii, *J. Appl. Phys.* 111 (2012) 114508.
- [5] Y. Noguchi, H. Lim, T. Isoshima, E. Ito, M. Hara, W.W. Chin, J.W. Han, H. Kinjo, Y. Ozawa, Y. Nakayama, H. Ishii, *Appl. Phys. Lett.* 102 (2013) 203306.
- [6] J. Frischeisen, D. Yokoyama, A. Endo, C. Adachi, W. Brütting, *Org. Electron.* 12 (2011) 809.
- [7] K.H. Kim, S. Lee, C.K. Moon, S.Y. Kim, Y.S. Park, J.H. Lee, J. Woo Lee, J. Huh, Y. You, J.J. Kim, *Nat. Commun.* 5 (2014) 4769.
- [8] S.Y. Kim, W.I. Jeong, C. Mayr, Y.S. Park, K.H. Kim, J.H. Lee, C.K. Moon, W. Brütting, J.J. Kim, *Adv. Funct. Mater.* 23 (2013) 3896.
- [9] D. Yokoyama, A. Sakaguchi, M. Suzuki, C. Adachi, *Appl. Phys. Lett.* 95 (2009) 243303.
- [10] D. Yokoyama, H. Sasabe, Y. Furukawa, C. Adachi, J. Kido, *Adv. Funct. Mater.* 21 (2011) 1375.
- [11] E. Ito, Y. Washizu, N. Hayashi, H. Ishii, N. Matsui, K. Tsuboi, Y. Ouchi, Y. Harima, K. Yamashita, K. Seki, *J. Appl. Phys.* 92 (2002) 7306.
- [12] D.Y. Kondakov, J.R. Sandifer, C.W. Tang, R.H. Young, *J. Appl. Phys.* 93 (2003) 1108.
- [13] V.V. Jarikov, D.Y. Kondakov, *J. Appl. Phys.* 105 (2009) 34905.
- [14] Y. Noguchi, H. Kim, R. Ishino, K. Goushi, C. Adachi, Y. Nakayama, H. Ishii, *Org. Electron.* 17 (2015) 184.
- [15] T.D. Schmidt, L. Jäger, Y. Noguchi, H. Ishii, W. Brütting, *J. Appl. Phys.* 117 (2015) 215502.
- [16] M.J. Jurow, C. Mayr, T.D. Schmidt, T. Lampe, P.I. Djurovich, W. Brütting, M.E. Thompson, *Nat. Mater.* 15 (2016) 85.
- [17] C. Mayr, W. Brütting, *Chem. Mater.* 27 (2015) 2749.
- [18] M. Shibata, Y. Sakai, D. Yokoyama, *J. Mater. Chem.* 3 (2015) 11178.
- [19] L. Jäger, T.D. Schmidt, W. Brütting, *AIP Adv.* 6 (2016) 095220.
- [20] T. Isoshima, Y. Okabayashi, E. Ito, M. Hara, W.W. Chin, J.W. Han, *Org. Electron.* 14 (2013) 1988.
- [21] N. Kajimoto, T. Manaka, M. Iwamoto, *J. Appl. Phys.* 100 (2006) 053707.
- [22] T. Miyamae, N. Takada, T. Yoshioka, S. Miyaguchi, H. Ohata, T. Tsutsui, *Chem. Phys. Lett.* 616–617 (2014) 86.
- [23] K. Kutzner, *Thin Solid Films* 14 (1972) 49.
- [24] L. Onsager, D. Staebler, S. Mascarenhas, *J. Chem. Phys.* 68 (1978) 3823.
- [25] J. Chrzanowski, B. Sujak, *Thin Solid Films* 79 (1981) 101.
- [26] M.J. Iedema, M.J. Dresser, D.L. Doering, J.B. Rowland, W.P. Hess, A.A. Tsekouras, J.P. Cowin, *J. Phys. Chem. B* 102 (1998) 9203.
- [27] A. Cassidy, O. Plekan, R. Balog, J. Dunger, D. Field, N.C. Jones, *J. Phys. Chem.* 118 (2014) 6615.
- [28] C. Bu, J. Shi, U. Raut, E.H. Mitchell, R.A. Baragiola, *J. Chem. Phys.* 142 (2015) 134702.
- [29] I.K. Gavra, A.N. Pilidi, A.A. Tsekouras, *J. Chem. Phys.* 146 (2017) 104701.
- [30] N. Hayashi, K. Imai, T. Suzuki, K. Kanai, Y. Ouchi, K. Seki, *IPAP Conf* (2004) 69.
- [31] C. Murawski, C. Elschner, S. Lenk, S. Reineke, M.C. Gather, *Org. Electron.* 53 (2018) 198.
- [32] H. Uoyama, K. Goushi, K. Shizu, H. Nomura, C. Adachi, *Nature* 492 (2012) 234.
- [33] H. Kaji, H. Suzuki, T. Fukushima, K. Shizu, K. Suzuki, S. Kubo, T. Komino, H. Oiwai, F. Suzuki, A. Wakamiya, Y. Murata, C. Adachi, *Nat. Commun.* 6 (2015) 8476.
- [34] K.H. Kim, C.K. Moon, J.W. Sun, B. Sim, J.J. Kim, *Adv. Opt. Mater.* 3 (2015) 895.
- [35] J.W. Sun, K.H. Kim, C.K. Moon, J.H. Lee, J.J. Kim, *ACS Appl. Mater. Interfaces* 8 (15) (2016) 9806.
- [36] D. Yokoyama, K. Nakayama, T. Otani, J. Kido, *Adv. Mater.* 24 (2012) 6368.
- [37] J.W. Sun, J.H. Lee, C.K. Moon, K.H. Kim, H. Shin, J.J. Kim, *Adv. Mater.* 26 (2014) 5684.
- [38] A. Graf, P. Liehm, C. Murawski, S. Hofmann, K. Leo, M.C. Gather, *J. Mater. Chem. C* 2 (2014) 10298.
- [39] D. Yokoyama, A. Sakaguchi, M. Suzuki, C. Adachi, *Org. Electron.* 10 (2009) 127.
- [40] T. Sawabe, I. Takasu, T. Ono, T. Yonehara, S. Enomoto, **US Patent, US20130069090 A1.**
- [41] M. Kröger, S. Hamwi, J. Meyer, T. Dobbertin, T. Riedl, W. Kowalsky, H.-H. Johannes, *Phys. Rev. B* 75 (2007) 235321.
- [42] Y. Okabayashi, E. Ito, T. Isoshima, M. Hara, *APEX* 5 (2012) 055601.
- [43] S.F. Boys, F. Bernardi, *Mol. Phys.* 19 (1970) 553.
- [44] S. Simon, M. Duran, J.J. Dannenberg, *J. Chem. Phys.* 105 (1996) 11024.
- [45] S. Altazin, S. Züfle, E. Knapp, C. Kirsch, T.D. Schmidt, L. Jäger, Y. Noguchi, W. Brütting, B. Ruhstaller, *Org. Electron.* 39 (2016) 244.
- [46] H. Kinjo, H. Lim, T. Sato, Y. Noguchi, Y. Nakayama, H. Ishii, *APEX* 9 (2016) 21601.
- [47] W. Brütting, S. Berleb, A.G. Mückl, *Org. Electron.* 2 (2001) 1.
- [48] B. Ruhstaller, S.A. Carter, S. Barth, H. Riel, W. Riess, J.C. Scott, *J. Appl. Phys.* 89 (2001) 4575.
- [49] H. Nakanotani, K. Masui, J. Nishide, T. Shibata, C. Adachi, *Sci. Rep.* 3 (2013) 2127.
- [50] J.H. Lee, S.W. Liu, C.-A. Huang, K.H. Yang, Y. Chang, *Proc. SPIE* 5464 (2004) 434.
- [51] P. Friederich, V. Rodin, F. von Wrochem, W. Wenzel, *ACS Appl. Mater. Interfaces* 10 (2018) 1881.